

Step-Shaped Cavity-Backed Antenna and Wideband Wide-Angle Impedance Matching in Planar Phased Array

Yaqing Wen*, Guoming Gao, and Wenjun Chen

Abstract—An improved wideband cavity-backed antenna and a planar phased array with wideband wide-angle impedance matching (WAIM) are provided in this paper. A step-shaped cavity is applied in the antenna, so the relative bandwidth of $VSWR < 2$ can be improved to more than 52% without increasing the cavity profile. Furthermore, a planar phased array constructed by the cavity-backed antenna can work with a wide-angle scanning range of $\pm 60^\circ$ at both E - and H -planes. Due to the wide-angle scanning range, the impedance matching for the phased array will be unstable in the required wideband. Consequently, the matching layer with metamaterials has been loaded on the phased array. The VSWR is controlled within 2 in E -plane and 3.5 in H -plane during the scanning range of $\pm 60^\circ$ in wide bandwidth.

1. INTRODUCTION

In recent years, multifunctional radar has been an important developing direction for the radar application. The wideband of radar is the primary condition for the diversification of radar operational tasks and functions. The scanning range of a phased array antenna, which is used in a radar system, is also a fundamental index for application [1]. For a airborne detection radar and shipborne omnidirectional coverage radar, wide-angle scanning property can effectively improve the combat capability of a radar. For instance, an AN/APG-81 active phased array on an F22 fighter can not only realize SAR two-dimensional mapping imaging, but also have the functions of moving target detection and communication of ground and sea targets. The wideband property and wide-angle scanning property are necessary means to achieve all these functions.

There are many ways to achieve wideband in a phased array, such as Vivaldi antenna phased array [2]. Phased array systems tend to be miniaturized and light weight, presently, which is reflected in the low profile and integration at the radiating end of the array. For a planar phased array, the cavity-backed antenna unit can effectively satisfy these requirements including the profile, bandwidth, and scanning range. The cavity-backed phased array antenna in [3] has a compact structure, which is also able to achieve wide-angle scanning. The bandwidth of the cavity-backed antenna can obtain 20% ~ 40% with a profile less than $\lambda_h/4$ (λ_h is the high frequency wavelength) [4–6]. A 64-element cavity-backed array is proposed in [4]. The bandwidth of the antenna embedded in the array is beyond 25%, and the scanning range could be $\pm 60^\circ$ at centre frequency. However, the grating lobe is generated with the low elevation angle scanning at high frequency.

In [3], SIW technology is used in a cavity-backed phased array antenna, whose scan performance in the E -plane is substantially better than that of conventional microstrip patch phased arrays. So, a cavity-backed phased array can obtain an excellent WAIM performance in the E -plane. However, for a phased array in a multifunctional radar, the WAIM performance needs also to be maintained in both the E - and H -planes with the wide bandwidth. For wide-angle scanning array antennas, the

Received 17 August 2019, Accepted 26 November 2019, Scheduled 22 December 2019

* Corresponding author: Yaqing Wen (yaqingwen@126.com).

The authors are with the No. 724 Institute of CSIC, Nanjing, China.

magnitude of the reflection changes substantially with the scan angle and wave polarization because of the coupling among the active elements [7, 8]. Scanning performance and aperture efficiency of the array can be improved with the periodic and aperiodic sparse arrays, which solves the problem of coupling among the active elements in the phased array [9–14]. In [14], a periodic sparse dipole array and cavity-backed antenna are used in combination, which can obtain unidirectional radiation patterns with high aperture efficiency. However, its application is limited by the narrow bandwidth and only one-dimensional scanning. In earlier antenna designs, monolayer or multilayer thin planar dielectric sheets covering the array surface has been proposed to meet the scanning range requirement [7, 8]. The dielectric sheet located above the array effectively acts as a shunt susceptance which is devoted to matching the active element radiated impedance with the air impedance at different steering angles. Ultimately, the power reflected by the air-antenna interface to the feeding network is minimized. In order to obtain the effective impedance matching layer in the wide-angle and wideband, metamaterial has been applied to the matching layer loaded on phased arrays [15–20]. Metamaterial is used to implement an anisotropic dielectric layer, which could achieve wide-angle impedance matching of a waveguide-fed planar phased array [15, 16]. Another kind of the split-ring resonators (SRRs) shaped metamaterials matching layer, which can rely on a magnetic vector normal to the array plane, is employed to improve the scanning characteristics of a dipole or slot phased array in the H - and D -planes [17, 18].

In this paper, a cavity-backed microstrip patch antenna has been designed with a bandwidth over X-band at first. Compared with the traditional rectangular hollow cavity, a stepped cavity is used in the proposed antenna for wider bandwidth. The bandwidth can be raised to more than 52% over X-band with the same height profile of $\lambda_h/4$. Then, a 64-elements (8×8) phased array with a metamaterials matching layer is analysed and fabricated. The simulated and measured results show that the phased array obtains wide-angle scanning and wide-angle impedance matching of $\pm 60^\circ$ in E - and H -planes during X-band. The phased array is designed for the low profile airborne radar.

2. ANTENNA DESIGN AND ANALYSIS

The structure of the proposed cavity-backed antenna shown in Fig. 1 is fabricated by three layers. The substrate is Arlon AD300 with $\epsilon_r = 3.0$ and $\delta_d = 2.0 \times 10^{-3}$. The thickness of the upper substrate is $h_1 = 2.0$ mm, and the thickness of the other substrate is $h_2 = 0.508$ mm. A rectangular patch is printed on the top center of the upper substrate with a size of $W \times L = 5.2$ mm \times 5.55 mm. The feeding microstrip line printed on the top of the under substrate excites the radiation patch by backed feeding. The feeding microstrip line holds a size of $W_f \times L_f = 1.05$ mm \times 7.35 mm. A circular patch is inserted on the feeding point of the microstrip line with a diameter of 1.4 mm. The metal backboard with the hollow cavity has a height of $h_g = 4.0$ mm, and the SSMP connector is embedded in the backboard. Besides, the whole height of the proposed antenna including the connector is $h_1 + h_2 + h_g = 6.508$ mm.

For a cavity-backed antenna, there are usually two forms of the hollow cavity. One is closed at the

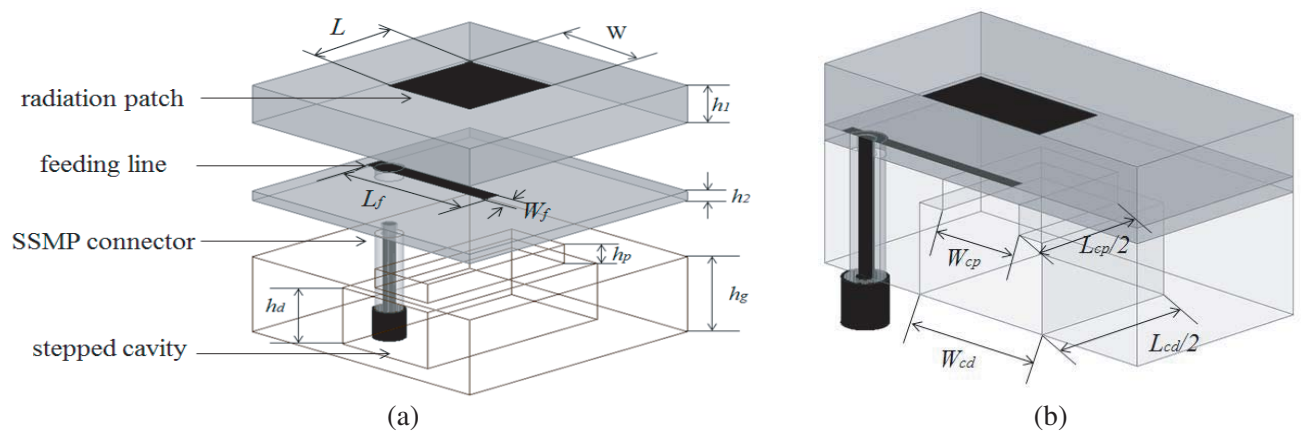


Figure 1. The structure of the proposed cavity-backed antenna. (a) Exploded view; (b) Section view.

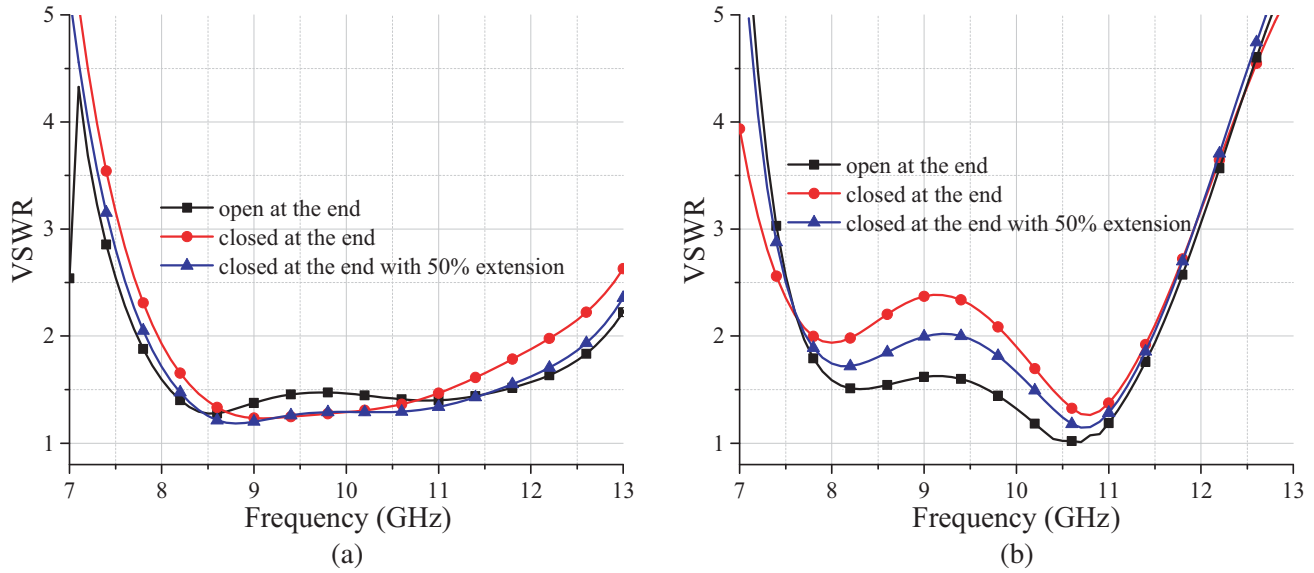


Figure 2. The simulated VSWR of the antenna with different structural forms at the end, (a) at periodic boundary; (b) at free space.

end, and the other is open at the end. To choose which kind of end of the hollow cavity, the antenna proposed in Fig. 1 is modified with a rectangular cavity with no step, which means $L_{cp} = L_{cd} = 8.4$ mm; $W_{cp} = W_{cd} = 3.1$ mm. Fig. 2 shows the simulated VSWR of the modified antenna at periodic boundary and at free space with different structural forms at the end. If the end of the cavity is closed, the reflected wave is generated in the cavity because of the metal boundary at the end. The electric currents on the patch and feeding line are influenced by the reflected wave, so the port matching is terrible in the band. While the end of the cavity is open, the reflected wave is reduced or weakened, which improves the impedance matching and bandwidth. However, the end-open cavity-backed antenna is usually not suitable for an integrated phased array system, which will affect the overall performance of a phased array system due to the electromagnetic interference on the components and digital circuits. In order for the closed-end cavity-backed antenna to achieve the good matching in a wideband, the depth of the cavity should be extended, which will increase the profile height of the array. These simulation results of the end-closed cavity with 50% extension in depth are shown in Fig. 2. However, due to the profile limitation, the extension in depth is not suitable.

So, in order to obtain wideband impedance matching of the closed-end cavity-backed antenna with the same profile height, the stepped cavity is used in the proposed antenna. A two-stepped cavity is shown in Fig. 1. The size of the stepped cavity increases from top to bottom. Due to the size increase of the cross section, the resonance characteristic is improved at the low frequency band. Meanwhile, with the size increase of the cavity, the electromagnetic wave decays gradually in the cavity. Therefore, the influence of the reflected wave on the impedance matching of the antenna will decrease, when the end of the cavity is closed. In summary, the impedance matching bandwidth of the antenna has been expanded on the premise of low profile and integration. The size of the top rectangular hollow cavity is $L_{cp} \times W_{cp} \times h_p = 8.4$ mm \times 3.3 mm \times 1 mm, and the bottom one is $L_{cd} \times W_{cd} \times h_d = 10.4$ mm \times 5.3 mm \times 3 mm. If a wider bandwidth is required for the antenna, the cavity with a three-stepped structure can be applied, and the profile height of the cavity remains unchanged. Fig. 3 shows the comparison of the simulated VSWR of the different stepped cavity-backed antenna at periodic boundary and free space. At periodic boundary, the one-stepped cavity-backed antenna, which refers to only a rectangular hollow cavity in the back, obtains a bandwidth of $VSWR < 2$ from 7.98 GHz to 12.22 GHz with a relative bandwidth of 42%. The two-stepped and three-stepped cavity-backed antennas can obtain bandwidths of $VSWR < 2$ from 7.58 GHz to 12.88 GHz and from 7.41 GHz to 12.99 GHz with the relative bandwidths of 52% and 55%, respectively. While the antennas are simulated at the free space, the impedance matching of the one-stepped cavity-backed antenna is

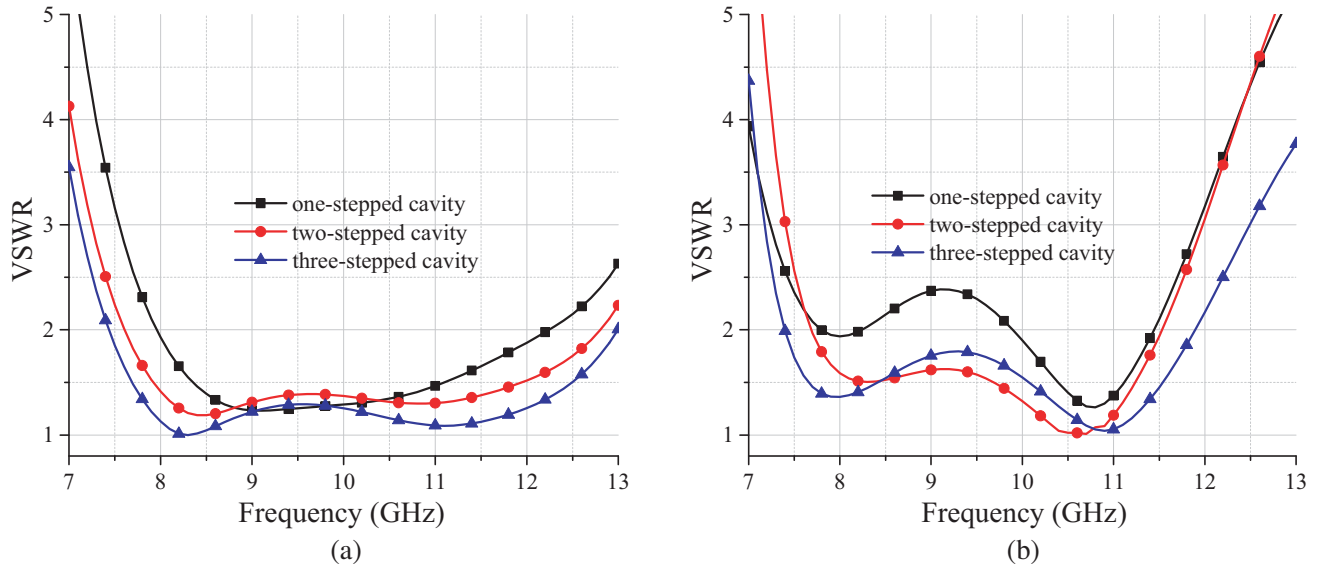


Figure 3. The comparison of the simulated VSWR of the different stepped cavity-backed antenna, (a) at periodic boundary; (b) at free space.

terrible in the band, and the VSWR is larger than 2. However, the two-stepped and three-stepped cavity-backed antennas can still obtain the bandwidths of $VSWR < 2$ from 7.66 GHz to 11.58 GHz and from 7.38 GHz to 11.89 GHz with the relative bandwidths of 41% and 47%, respectively. Hence, the impedance matching and bandwidth are improved when a stepped cavity is applied to the antenna at both the periodic boundary and free space. A two-stepped cavity-backed antenna is used for phased array construction in this paper.

The radiation patterns of the designed two-stepped cavity-backed antenna are nearly the same in the X-band. Fig. 4 shows the simulated radiation patterns of the two-stepped cavity-backed antenna at some specific frequencies. The peak gain of the antenna ranges from 5.45 dBi to 6.54 dBi during the band. Meanwhile, the relative gain of cro-polarization is lower than -50 dB at E -plane and -20 dB at H -plane.

3. ANALYSIS OF THE WAIM

For the phased array, the scanning impedance varies with the scanning angle. This phenomenon can be observed from the generation of the surface current on the interface between radiation layer and free space. The surface impedance at the interface is determined by the boundary of voltage continuity and surface current continuity. The E -plane and H -plane surface impedances at a dielectric-to-air interface are influenced by the incident wave angle.

In the infinite current layer theory of the Wheeler's research, it is shown that when the radiation angle changes, the radiation resistance of the phased array will change, and the law is the projection area of the plane wave on the aperture [6]. The reflection angle of plane wave is opposite to the incident angle. For the E -plane, when the plane wave is obliquely incident to the surface, the length of the current layer according to the plane wave projection increases from the point of view of the incident wave, and the impedance increases as a result. The VSWR is,

$$\rho_E = \frac{1/\cos\theta - 1}{1/\cos\theta + 1} = \tan^2\theta/2 \quad (1)$$

For the H -plane, when the plane wave is obliquely incident to the surface, the thickness of the current layer according to the plane wave projection increases from the point of view of the incident

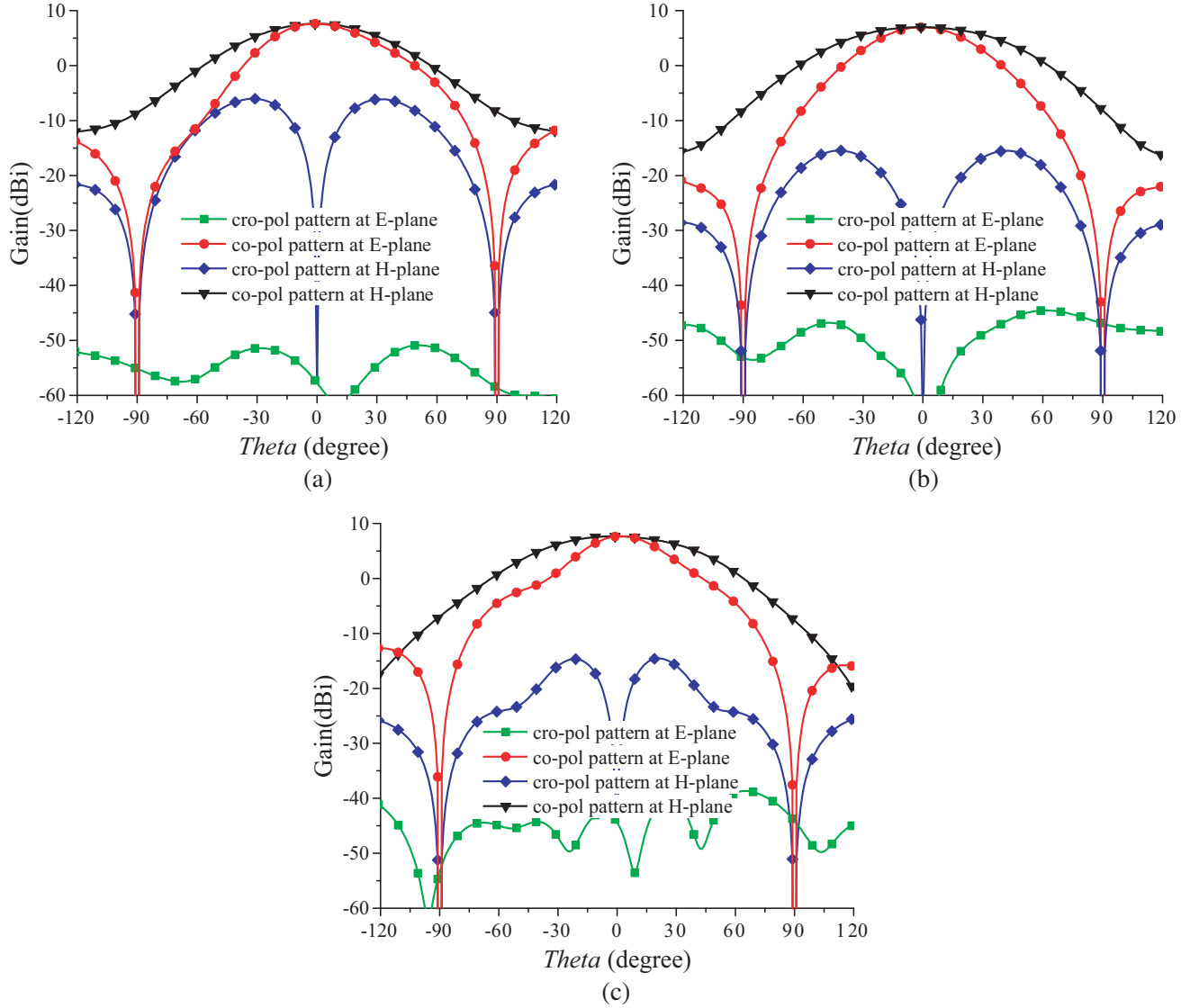


Figure 4. The simulated radiation patterns of the two-stepped cavity-backed antenna, (a) 8 GHz; (b) 10 GHz; (c) 12 GHz.

wave, and the impedance increases as a result. The VSWR is,

$$\rho_H = \frac{\cos \theta - 1}{\cos \theta + 1} = -\tan^2 \theta / 2 \tag{2}$$

The above results are obtained from the view of receiving plane wave for the phased array, and the results obtained from the view of the transmitting plane wave from the phased array front are the reciprocal of the above results. The change of the impedance varies with incident wave angles, in addition with the change of the projection area from the wavefront to the array front; on the other hand, it is related to the radiation unit. For the unit arranged uniformly in the infinite array, the radiation impedance is,

$$R_0 = \frac{R_s \cdot l^2}{d^2 \cos \theta} \tag{3}$$

R_s is the impedance of the free space of 377Ω , l the length of the current source, d the length of the unit, and θ the scanning angle. For the source in the array factor, the pattern is $\cos \theta$ and 1 at E -plane

and H -plane, respectively. Therefore, the scanning impedances at E -plane and H -plane are,

$$R_E/R_0 = \frac{[f_E(\theta)]^2}{\cos \theta} = \cos \theta \quad (4)$$

$$R_H/R_0 = \frac{[f_H(\theta)]^2}{\cos \theta} = 1/\cos \theta \quad (5)$$

So, the trends of the scanning impedances at the E -plane and H -plane are opposite with the change of scanning angle. Simultaneously, the change of the impedance causes mismatching in the wide-angle scanning range for the phased array antenna.

The traditional method to improve the WAIM in phased array systems is to add one or more isotropic planar dielectric layers among the radiation surface and space free [7]. However, because of the difference of the trends of the surface impedances between the E -plane and H -plane, this method cannot get good effects on both planes simultaneously. Fig. 5 shows the active VSWR of the unit in the

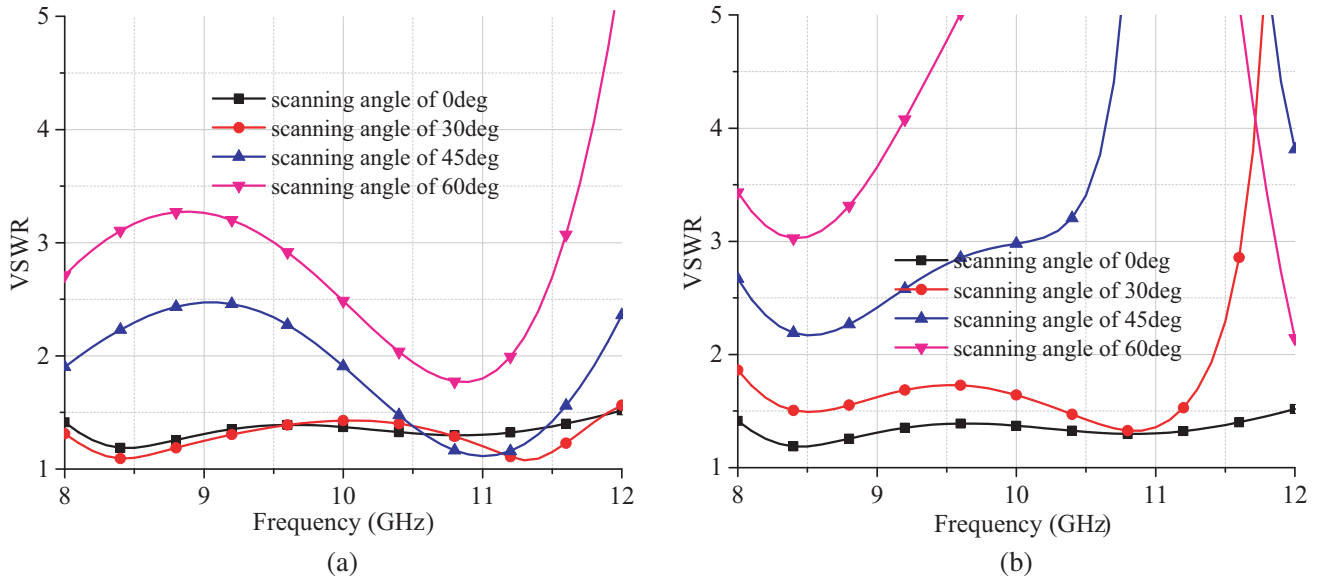


Figure 5. The simulated active VSWR of the unit in the infinite phased array, (a) at E -plane; (b) at H -plane.

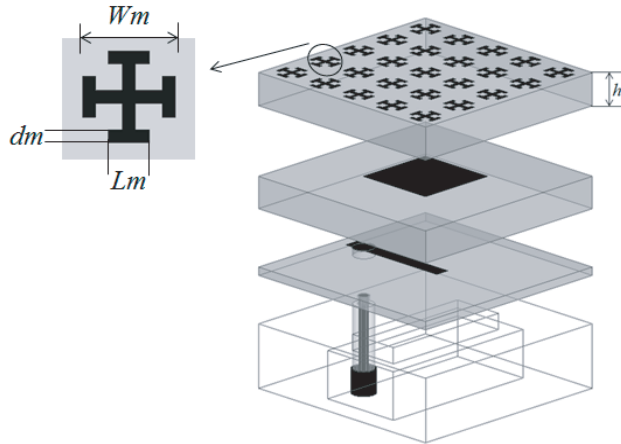


Figure 6. The structure of the proposed cavity-backed antenna with the matching layer based on Jerusalem cross.

infinite phased array, which is constituted by the two-stepped cavity-backed antenna proposed above. There is obvious mismatching for the active VSWR at large scanning angles.

The metamaterial can equivalently function as the anisotropic dielectric, which can work as the WAIM layer [15,19]. Compared to the traditional isotropic dielectric, the metamaterial layer can effectively act for the impedance matching on both E -plane and H -plane. In order to solve the impedance matching problem during wide-angle scanning, the matching layer based on a Jerusalem cross is designed on the proposed antenna. The radiation impedance and parameters of the anisotropic dielectric are according to the method in [15,19]. Fig. 6 shows the structure of the antenna with the matching layer. The Jerusalem cross is fabricated on a substrate of Rogers 5880 with thickness $hm = 2.0$ mm. The distances between the two cross units in both E -plane and H -plane are 2.6 mm. The lengths of the cross are $Wm = 1.75$ mm and $Lm = 0.78$ mm, and the width of the cross is $dm = 0.25$ mm.

The active VSWRs of the unit in the infinite phased array constituted by the two-stepped cavity-

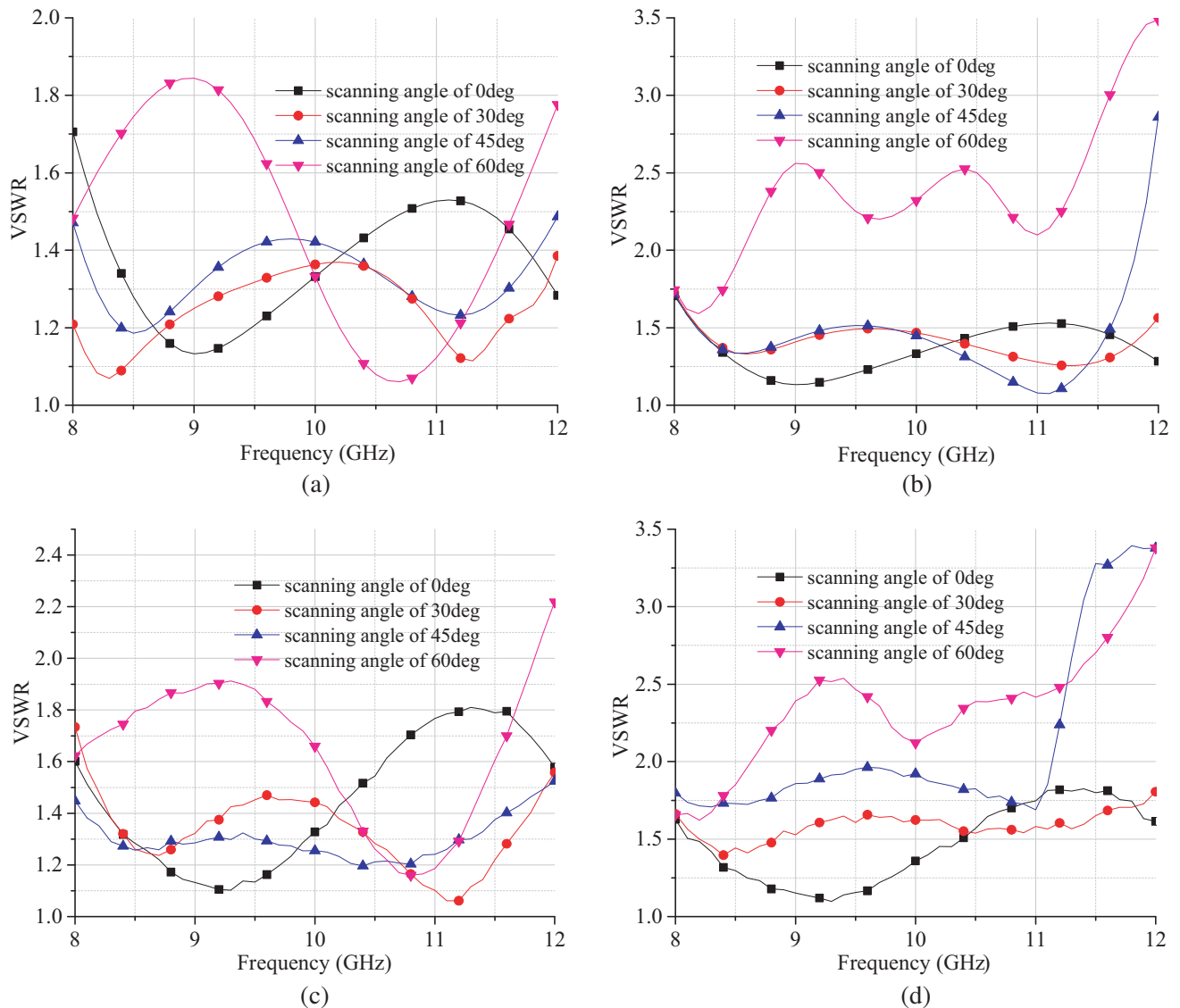


Figure 7. The simulated and measured active VSWR of the unit in the phased array with the matching layer, (a) simulated results at E -plane; (b) simulated results at H -plane; (c) measured results at E -plane; (d) measured results at H -plane.

backed antenna with the matching layer are simulated as in Figs. 7(a) and (b), and the active VSWRs of the unit in the center of the 8×8 array of the same structure are measured as in Figs. 7(c) and (d). The active VSWRs are under 2 and 3.5 in the wide-angle scanning range of $\pm 60^\circ$ at E -plane and H -plane, respectively. The measured results are consistent with the simulated ones.

4. SCANNING PATTERN RESULTS AND ANALYSIS

An 8×8 planar phased array is fabricated with the element antenna proposed above. The phased array works in the X-band. Therefore, considering the grating lobe condition and broadband characteristic of the phased array, the cell space between the adjacent elements is determined by $13 \text{ mm} \times 13 \text{ mm}$. The phased array has been fabricated. The simulated model of the phased array and a photograph of the fabricated structure are shown in Fig. 8. The array measured in an anechoic chamber and the measurement system for the scanning radiation patterns is set up by using coaxial cables, six-bit digital phase shifters, power dividers, and a computer. The measurement system is the same as the one in [21].

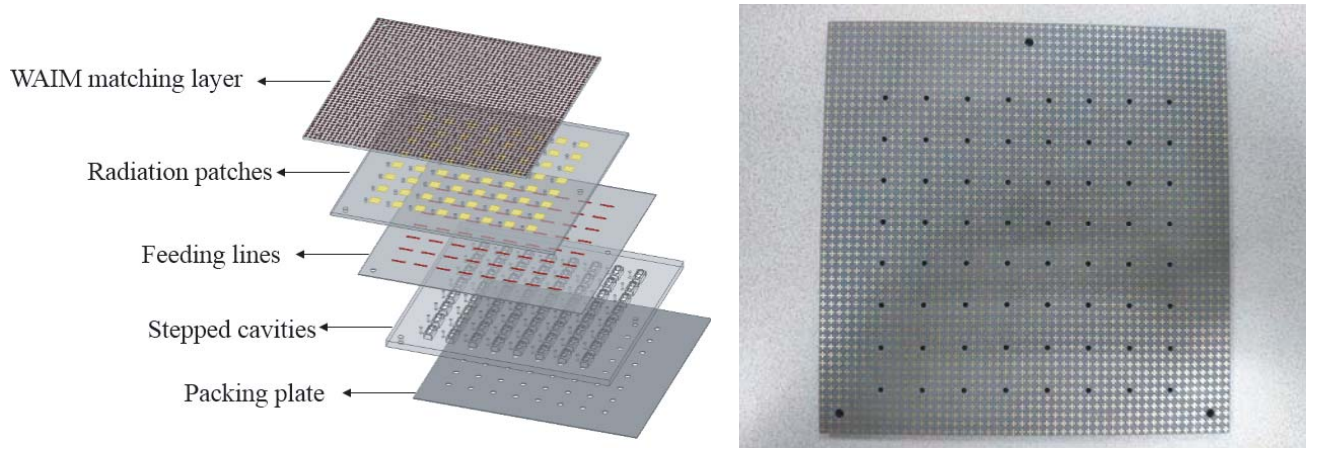


Figure 8. The simulated model of the phased array and the photograph of fabricated structure.

Figure 7 indicates that the elements obtain excellent impedance matching in the wide-angle scanning at both E -plane and H -plane. Therefore, the phased array can scan its main lobe in a wide-angle range at both E -plane and H -plane. Fig. 9 shows the measured scanning radiation pattern of the phased array at different frequencies at both E -plane and H -plane.

Table 1. Comparison of the proposed antenna and some previous works.

	Maximum gain (dBi)	Scanning range ($^\circ$)	Bandwidth	Type of the antenna
This work	6.54 for element 23.2 for array	± 60	52%	8×8 two-stepped cavity-backed antenna
[3]	-	60	12%	7×7 SIW cavity-backed patch antenna
[4]	5 for element	± 60	25%	8×8 rectangular hollow-cavity antenna
[5]	8.6 for element	-	70%	cavity-backed aperture antenna
[6]	-	± 60	44.35%	2×18 cavity-backed array
[13]	About 18 for array	± 60	100% (VSWR < 3)	8×8 tightly coupled dipole

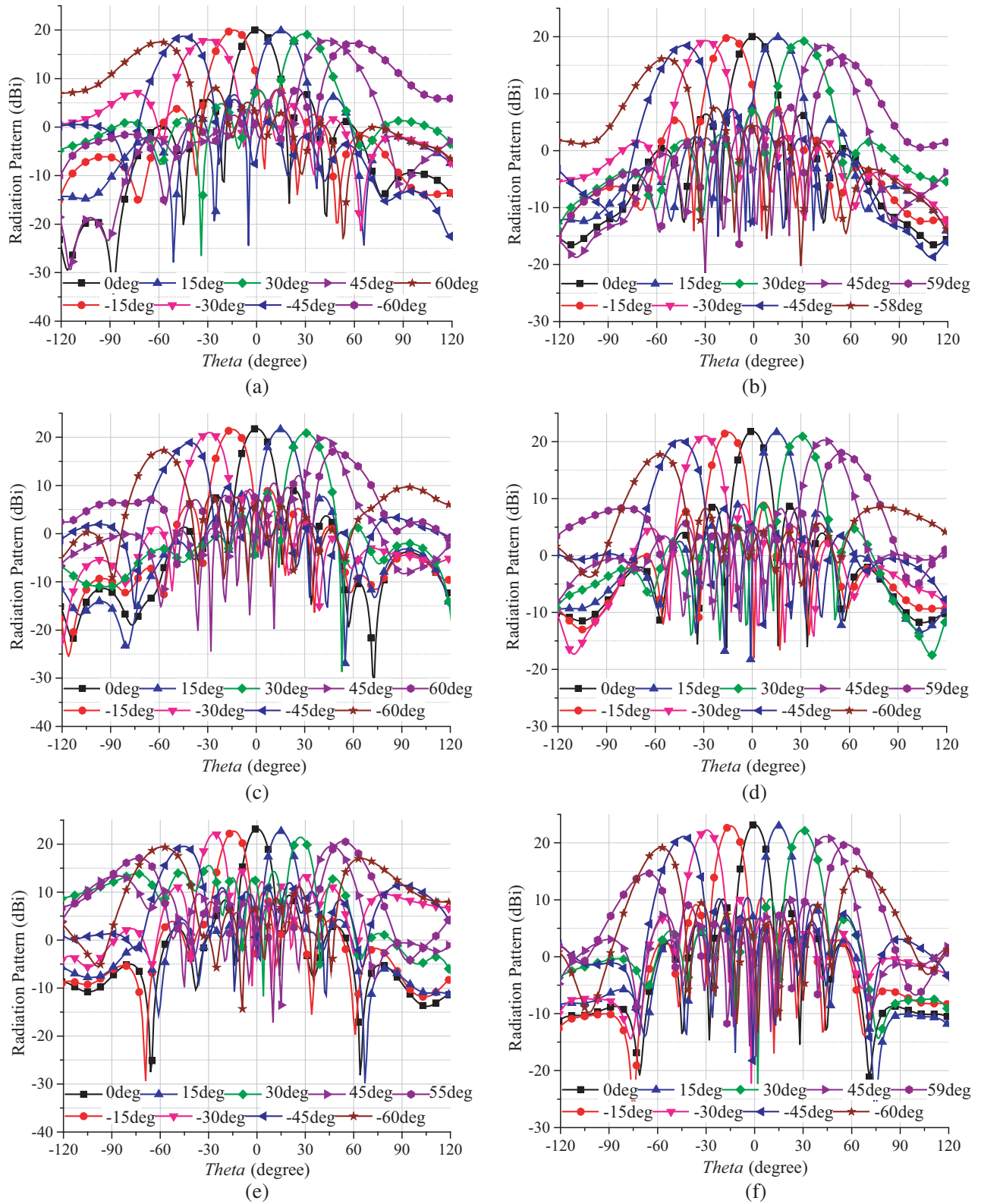


Figure 9. The measured scanning radiation pattern of the phased array with the matching layer, (a) 8 GHz at *E*-plane; (b) 8 GHz at *H*-plane; (c) 10 GHz at *E*-plane; (d) 10 GHz at *H*-plane; (e) 12 GHz at *E*-plane; (f) 12 GHz at *H*-plane.

In Fig. 9, we can see that the phased array holds the scanning range of $\pm 60^\circ$ at both E -plane and H -plane in the X-band. Meanwhile, the maximum gain varies from 23.2 dBi to 19.8 dBi in the X-band. The SLL is less than -10 dB in most scanning range. The gain fluctuation in the scanning range is less than 3.6 dB at E -plane and 4.4 dB at H -plane, respectively, in the X-band.

For comparison, the performance of the proposed antenna and some previous works are presented in Table 1. The proposed phased array antenna can achieve much wider bandwidth than the antennas in [3, 4, 6]. Compared with the antenna in [5], the proposed antenna is better applied to the phased array. The proposed antenna can achieve higher gain and better impedance matching than [13].

5. CONCLUSION

In this paper, an improved cavity-backed antenna with wideband is proposed. The application of the stepped cavity ensures that the antenna can obtain a bandwidth more than 52% with the profile unchanged and with closed-end. It is beneficial to the miniaturization design and integration of the plane phased array. The simulated results also indicate that the radiation patterns get an excellent consistency in the working band with low cro-polarization at both E -plane and H -plane. A matching layer with the structure of a Jerusalem cross is designed and added on the antenna, in order to get a wide-angle impedance matching when the phased array scans the main lobes at both E -plane and H -plane. An 8×8 planar phased array is designed and fabricated using the developed element. The beam scanning is realized in a wide-angle range of $\pm 60^\circ$ in both E -plane and H -plane in wideband.

REFERENCES

1. Mailloux, R. J., *Phased Array Antenna Handbook*, 2nd Edition, Artech House Antennas and Propagation Library, Artech Print on Demand, Norwood, MA, USA, 2008.
2. Balanis, C. A., *Antenna Theory, Analysis and Design*, 2nd Edition, Wiley, New York, NY, USA, 1997.
3. Awida, M. H., A. H. Kamel, and A. E. Fathy, "Analysis and design of wide-scan angle wideband phased arrays of substrate-integrated cavity-backed patches," *IEEE Trans. Antennas Propag.*, Vol. 61, No. 6, 3034–3041, Jun. 2013.
4. Ding, Z. F., S. Q. Xiao, C. R. Liu, M. C. Tang, C. Zhang, and B. Z. Wang, "Design of a broadband, wide-beam hollow cavity multilayer antenna for phased array applications," *IEEE Antennas Wireless Propag. Lett.*, Vol. 15, 1040–1043, 2016.
5. Yang, W. W. and J. Y. Zhou, "Wideband circularly polarized cavity-backed aperture antenna with a parasitic square patch," *IEEE Antennas Wireless Propag. Lett.*, Vol. 13, 197–200, 2014.
6. Xia, R.-L., S.-W. Qu, S. W. Yang, and Y. Chen, "Wideband wide-scanning phased array with connected backed cavities and parasitic striplines," *IEEE Trans. Antennas Propag.*, Vol. 66, No. 4, 1767–1775, Apr. 2018.
7. Magill, E. and H. A. Wheeler, "Wide-angle impedance matching of a planar array antenna by a dielectric sheet," *IEEE Trans. Antennas Propag.*, Vol. 14, No. 1, 49–53, Jan. 1966.
8. Chen, C. C., "Broad-band impedance matching of rectangular waveguide phased arrays," *IEEE Trans. Antennas Propag.*, Vol. 21, No. 3, 298–302, May 1973.
9. Oliveri, G. and A. Massa, "Bayesian compressive sampling for pattern synthesis with maximally sparse non-uniform linear arrays," *IEEE Trans. Antennas Propag.*, Vol. 59, No. 2, 467–481, Feb. 2011.
10. Oliveri, G., M. Carlin, and A. Massa, "Complex-weight sparse linear array synthesis by Bayesian compressive sampling," *IEEE Trans. Antennas Propag.*, Vol. 60, No. 5, 2309–2326, May 2012.
11. Qu, S. W., D. J. He, S. W. Yang, and Z. P. Nie, "Novel parasitic microstrip arrays for low-cost active phased array applications," *IEEE Trans. Antennas Propag.*, Vol. 62, No. 4, 1731–1737, Apr. 2014.
12. Qu, S. W., D. J. He, M. Y. Xiao, Z. P. Nie, and C. H. Chan, "High efficiency periodic sparse patch array based on mutual coupling," *IEEE Antennas Wireless Propag. Lett.*, Vol. 10, 1317–1320, 2011.

13. Qu, S. W., P. F. Li, R. L. Xia, S. W. Yang, J. Hu, and Z. P. Nie, "Low-cost periodic sparse cavity-backed phased array based on multiport elements," *IEEE Trans. Antennas Propag.*, Vol. 63, No. 9, 4175–4179, Sept. 2015.
14. Xiao, S. W., S. W. Yang, H. Y. Zhang, Q. S. Xiao, Y. K. Chen, and S. W. Qu, "Practical implementation of wideband and wide-scanning cylindrically conformal phased array," *IEEE Trans. Antennas Propag.*, Vol. 67, No. 8, 5729–5733, Aug. 2019.
15. Oliveri, G., F. Viani, N. Anselmi, and A. Massa, "Synthesis of multilayer WAIM coatings for planar-phased arrays within the system-by-design framework," *IEEE Trans. Antennas Propag.*, Vol. 63, No. 6, 2482–2496, Jun. 2015.
16. Sajuyigbe, S., et al., "Wide angle impedance matching metamaterials for waveguide-fed phased-array antennas," *IET Microw. Antennas Propag.*, Vol. 4, No. 8, 1063–1072, Aug. 2010.
17. Cameron, T. R. and V. George, "Eleftheriades analysis and characterization of a wide-angle impedance matching metasurface for dipole phased arrays," *IEEE Trans. Antennas Propag.*, Vol. 65, No. 9, 3928–3938, Sept. 2015.
18. Cameron, T. R. and V. George, "Experimental validation of a wideband metasurface for wide-angle scanning leaky-wave antennas," *IEEE Trans. Antennas Propag.*, Vol. 65, No. 10, 5245–5256, Oct. 2017.
19. Jiang, Z. H., J. A. Bossard, X. Wang, and D. H. Werner, "Synthesizing metamaterials with angularly independent effective medium properties based on an anisotropic parameter retrieval technique coupled with a genetic algorithm," *J. Appl. Phys.*, Vol. 109, No. 1, 013515, Jan. 2011.
20. Zou, W.-M., S.-W. Qu, and S. W. Yang, "Wideband wide-scanning phased array in triangular lattice with electromagnetic band-gap structures," *IEEE Trans. Antennas Propag.*, Vol. 18, No. 3, 422–426, Mar. 2019.
21. Wen, Y.-Q., B.-Z. Wang, and X. Ding, "A wide-angle scanning and low sidelobe level microstrip phased array based on genetic algorithm optimization," *IEEE Trans. Antennas Propag.*, Vol. 64, No. 2, Feb. 2016.